

## FLUXES OF NITROGEN OXIDES OVER A TEMPERATE DECIDUOUS FOREST

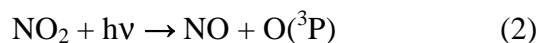
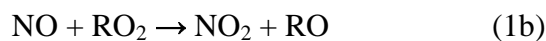
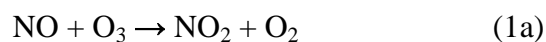
C. V. Horii, J. W. Munger, S. C. Wofsy, M. Zahniser, D. Nelson, J. B. McManus

### ABSTRACT

Eddy covariance flux measurements of NO, NO<sub>2</sub>, and O<sub>3</sub> were obtained above the mixed deciduous canopy at Harvard Forest in central Massachusetts from April to November 2000. Net deposition of NO<sub>x</sub> was observed regardless of time of day or season, with average velocity of ~0.2 cm s<sup>-1</sup>. At night, NO<sub>2</sub> is deposited at a rate that depends nonlinearly on NO<sub>2</sub> concentration and cannot be explained by N<sub>2</sub>O<sub>5</sub> hydrolysis, suggesting HONO formation by heterogeneous disproportionation of NO<sub>2</sub>. During the day, photochemically driven NO<sub>x</sub> fluxes conform to the predicted behavior based on gradients of light and eddy diffusivity through the canopy, with residual net flux attributable to both non-foliar and stomatal processes. The results were consistent with a compensation point for NO<sub>2</sub> near 1.5 nmol mol<sup>-1</sup>. These results were confirmed by independent evidence from NO, NO<sub>2</sub>, and O<sub>3</sub> profiles acquired at the site over several years. The observed NO<sub>x</sub> deposition has the greatest potential impact on tropospheric chemistry during the night and winter, when mixing depths are shallow and chemical NO<sub>x</sub> oxidation is slow. The results contradict widely used parameterizations of NO<sub>2</sub> deposition that both overestimate stomatal uptake and do not allow for surface uptake when stomates are closed.

### INTRODUCTION

Tropospheric NO<sub>2</sub> is the critical nitrogen oxide radical in the photochemical formation of O<sub>3</sub>. The NO<sub>x</sub> species, NO and NO<sub>2</sub>, rapidly interconvert in fast photochemical reactions (1)-(3). The cycle 1a, 2, and 3 has no net effect on O<sub>3</sub>, but the sequence 1b, 2, and 3 produces O<sub>3</sub>.



Production of  $\text{O}_3$  is limited by removal of  $\text{NO}_2$ , either by chemical reactions to make the non-radical species  $\text{HNO}_3$ , or by deposition to the surface. Chemical removal during the day is mainly due to reaction of  $\text{NO}_2$  with OH radicals, while at night removal proceeds via reaction with  $\text{O}_3$  to make the nitrate radical ( $\text{NO}_3$ ), which reacts with  $\text{NO}_2$  to form  $\text{N}_2\text{O}_5$  that can hydrolyze to  $\text{HNO}_3$ . These chain-terminating steps are slow compared to the chain propagating reactions (1)-(3), allowing one molecule of  $\text{NO}_x$  to be cycled many times before removal. Up to 100 molecules of  $\text{O}_3$  may be generated for each  $\text{NO}_x$  molecule entering the remote troposphere, with  $\sim 5$   $\text{O}_3$  thought to be typically produced per unit  $\text{NO}_x$  in the rural Eastern US [Liu et al., 1987; Hirsch et al., 1996].

Deposition of  $\text{NO}_2$  to surfaces bypasses atmospheric oxidation to  $\text{HNO}_3$  and reduces the amount of  $\text{NO}_x$  exported to the remote troposphere, thus potentially reducing tropospheric  $\text{O}_3$  production even if  $\text{NO}_2$  deposition constitutes a small fraction of the total flux of fixed N to the surface [Jacob et al., 1993; Liang et al., 1998]. Chamber studies have reported significant rates for uptake of  $\text{NO}_x$  radicals by vegetation, often attributed to  $\text{NO}_2$  deposition through stomates on foliar surfaces, as well as deposition to the forest floor and soils [Eugster and Hesterberg, 1996; Hanson and Lindberg, 1991]. These studies generally used high concentrations of  $\text{NO}_2$ . Extrapolation of the results to ambient concentrations suggests the presence of a compensation point ( $1\text{-}3 \text{ nmol mol}^{-1}$ )\*. When ambient concentrations fall below this concentration, leaves may

---

\* We use SI units for mixing ratio concentrations of trace gases in air, e.g.  $1 \text{ nmol mol}^{-1} = 1 \text{ ppbv}$  [Taylor, 1995].

begin to emit  $\text{NO}_2$  [e.g. Rondon et al., 1993; Sparks et al., 2001]. Release of  $\text{NO}_2$  by vegetation, if it occurs in nature, could significantly elevate global  $\text{O}_3$  production rates because  $\text{NO}_x$  concentrations are lower than the inferred compensation point over much of the globe [Lerdau et al., 2000].

$\text{NO}$  does not readily combine with atmospheric radicals to make stable non-radicals, and it is not expected to deposit to surfaces in significant amounts, though there is very little experimental confirmation [Hanson and Lindberg, 1991; Wesely and Hicks, 2000].  $\text{NO}$  is emitted from soils, typically at low rates in temperate forests [Williams et al., 1992; Munger et al., 1996]. Nevertheless rapid photochemical exchange between  $\text{NO}$ ,  $\text{O}_3$  and  $\text{NO}_2$  make simultaneous quantification of fluxes for these species a requirement for elucidating  $\text{NO}_x$  deposition rates [Fitzjarrald and Lenschow, 1983].

We present here  $\text{NO}$  and  $\text{NO}_2$  eddy covariance fluxes at the Harvard Forest Environmental Measurement Site for spring through fall, 2000, augmented by 12 years of data at the site for vertical profiles of  $\text{NO}_2$  and  $\text{NO}$  concentrations and eddy covariance fluxes of  $\text{O}_3$  and  $\text{NO}_y$ . The measurements represent the first simultaneous data for fluxes of  $\text{NO}$ ,  $\text{NO}_2$ , and  $\text{O}_3$  above a tall forest canopy with chemically specific eddy covariance instrumentation. The results allow us to critically test current assumptions about deposition and emission fluxes of  $\text{NO}_x$ .

Flux data and vertical profiles both showed significant  $\text{NO}_2$  deposition at night, including clean-air conditions. The results contradict widely used parameterizations of  $\text{NO}_2$  deposition (e.g., big-leaf, resistance-in-series models, following Wesely [1989] scheme) that do not provide for surface uptake when stomates are closed. Deposition fluxes increased nonlinearly with concentration, suggesting a chemical mechanism possibly involving production of  $\text{HONO}$  and  $\text{HNO}_3$  on leaf and soil surfaces. Photochemical cycling during the day led to equal and opposite

fluxes of NO (downward) and NO<sub>2</sub> (upward), driven by gradients in light and eddy diffusivity through the forest canopy. There was a residual net downward NO<sub>x</sub> flux during the day, with median deposition velocity of  $\sim 0.2 \text{ cm s}^{-1}$ , and a small upward flux of NO<sub>2</sub> that correlated with stomatal conductance. The results suggest very small daytime deposition of NO<sub>x</sub> for low NO<sub>2</sub> concentrations, with significant net deposition under polluted conditions.

## METHODS

We studied a 50-70-year old mixed deciduous forest of red oak and red maple, with scattered hemlock, red and white pine at Harvard Forest in central Massachusetts (42.54N, 72.18W; elevation, 340 m). The landscape is  $\sim 95\%$  forested and moderately hilly; the distance to the closest paved road is  $> 1.5 \text{ km}$ , and to the nearest small town  $> 10 \text{ km}$ . Two wind directions dominate: northwest flows bring relatively cool, dry, unpolluted air, and southwest winds bring warm, humid, significantly more polluted air [Moody et al., 1998; Munger et al. 1996]. We utilized two towers for this study: a permanent 30m Rohn 25G tower, used since 1990 to measure eddy fluxes of CO<sub>2</sub>, NO<sub>y</sub>, and O<sub>3</sub>, along with vertical profiles of NO, NO<sub>2</sub>, O<sub>3</sub>, and other species; and a temporary steel scaffolding tower, 23 m high (just above the top of the canopy), situated about 100 m to the SE and outfitted with a sonic anemometer and a Tunable Diode Laser Absorption Spectrometer (TDLAS) configured to measure eddy covariance fluxes and concentrations of NO<sub>2</sub> and concentrations of HNO<sub>3</sub> [Horii 2002]. Data from the two towers were matched and averaged into an hourly dataset, available at <http://www-as.harvard.edu/chemistry/index.html>.

*NO<sub>x</sub> Photolysis-Chemiluminescence (P-C) Measurements.* The P-C system measures NO and NO<sub>2</sub> concentration profiles at heights of 29, 24.1, 18.3, 12.7, 7.5, 4.5, 0.8, and 0.3 m on the

permanent tower [Munger et al. 1996]. From late August to mid-October 2000, it was reconfigured to measure NO concentrations at 10 Hz at the 29 m sampling height in order to determine eddy covariance fluxes for NO. Calibrations were made using standard gas mixtures for NO and NO<sub>2</sub>, traceable to NIST. The NO<sub>2</sub> and NO standards were cross-calibrated by titrating the NO standard with O<sub>3</sub> and by analyzing both using the NO<sub>y</sub> detector equipped with a hot gold catalyst for reducing NO<sub>y</sub> to NO.

*NO<sub>2</sub> TDLAS Measurements.* The TDLAS [Horii et al. 1999; Horii 2002] ran two diodes simultaneously from April through November 2000. One channel measured NO<sub>2</sub> concentrations at 1 Hz and the other measured concentrations of HNO<sub>3</sub>. The transition line strengths and pressure broadening coefficients used to compute absorption cross sections were obtained from the HITRAN spectral database [Rothman et al., 1998]. TDLAS calibration relied on independent laboratory determination of spectroscopic parameters (light path length, laser mode purity and frequency, laser tuning rate function, and laser line width), which were also checked in the field periodically using standard additions of HNO<sub>3</sub> and NO<sub>2</sub>, ambient water vapor, and a Germanium etalon. Multiple levels of cross-calibration were maintained throughout the experiment. Independent cross checks were obtained by comparing concentrations of H<sub>2</sub>O inferred using spectral lines in the both the NO<sub>2</sub> and HNO<sub>3</sub> spectral ranges (1590 and 1720 cm<sup>-1</sup> respectively) with H<sub>2</sub>O data from hygrometers on the main tower. Concentrations of NO<sub>2</sub> were directly compared during 459 hours of concurrent (4 April to 29 August 2000) measurements; the orthogonal distance regression of hourly data for the TDLAS vs. P-C had a slope of 1.1±0.2 (95% confidence interval, R<sup>2</sup>=0.91) and an intercept indistinguishable from zero [Horii 2002].

*O<sub>3</sub> UV Absorbance and Chemiluminescence Measurements.* O<sub>3</sub> concentration profiles and eddy covariance flux measurements on the main tower employ UV absorbance (Dasibi 1003AH,

sampling at the same heights as above) and C<sub>2</sub>H<sub>4</sub>-chemiluminescence (29 m sampling height), respectively [Munger et al. 1996].

*Micrometeorology and Auxiliary Measurements.* Triaxial sonic anemometers were oriented westward at the eddy covariance sampling height on each tower; data for vertical and horizontal wind velocities and virtual temperatures were acquired at 10 Hz to compute eddy covariance fluxes of heat, momentum, NO, and NO<sub>2</sub>, and at 5 Hz for O<sub>3</sub> [Munger et al. 1996, 1998]. Photosynthetic photon flux density (PPFD, 400-700nm) was measured continuously at 29 m on the main tower using a LI-COR quantum sensor.

*Eddy Covariance Fluxes.* We computed 30-minute mean fluxes of trace gases from the covariance of linearly detrended time series for vertical velocity ( $w'$ ) and trace gas concentrations ( $C'$ ). To correct for relatively slow instrument response times, data for virtual temperature and  $w$  were processed using instantaneous measurements by the sonic anemometer, then repeated using a set of single-pole low-pass numerical filters matched with the with the time response of each gas sensor. The ratio of the “filtered” heat flux for each 30-minute interval to the unfiltered heat flux provided an estimate of flux lost by instrumental smoothing of high-frequency fluctuations [Goulden et al., 1996; Munger et al., 1996; 1998]. Corrections were typically 20% or smaller for all species.

## RESULTS AND DISCUSSION

Figure 1 shows median values at each hour of the day for NO, NO<sub>2</sub>, and O<sub>3</sub> concentrations (upper panels) and fluxes (lower panels) for April through November 2000, segregated by wind sector. Photochemical production of NO during the day, and conversion to NO<sub>2</sub> at night, are apparent (*upper panels*). Concentrations of O<sub>3</sub> are typically much greater than

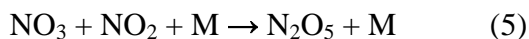
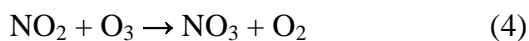
$\text{NO}_x$ , thus vertical  $\text{O}_3$  gradients and fluxes are regulated by ambient atmospheric concentrations and surface deposition, not by photochemical reactions with  $\text{NO}_x$  [Munger et al., 1996].

*Nighttime fluxes.* We observed downward fluxes of  $\text{NO}_2$  during all measurement seasons in 2000 (spring, summer, and fall) at night, for both clean (NW) and polluted (SW) wind sectors (Figure 1, lower panels). The downward nighttime  $\text{NO}_2$  flux increases with  $\text{NO}_2$  concentration, particularly at the highest ambient concentrations (Figure 2). The polynomial regression function  $F_{\text{NO}_2} = V_0 [\text{NO}_2] + a [\text{NO}_2]^2$  applied to hourly nighttime data yields:  $R^2 = 0.60$ ,  $V_0 = -0.08 \pm 0.03$  ( $p = 0.01$ ), and  $a = -0.013 \pm 0.001$  ( $p < 0.0001$ ). The quadratic dependence in the regression is largely driven by the two nights during the sampling period when the median concentration of  $\text{NO}_2$  exceeded  $10 \text{ nmol mol}^{-1}$ ; excluding these nights, neither the overall fit nor the coefficient  $a$  is statistically significant. However, even for concentrations below  $10 \text{ nmol mol}^{-1}$ , the coefficient  $V_0$  is negative and significant ( $V_0 = -0.16 \pm 0.06$ ,  $p = 0.005$ ). The regression suggests that the nighttime deposition velocity of  $\text{NO}_2$  ( $V_d(\text{NO}_2) = -F_{\text{NO}_2}/[\text{NO}_2]$ ) increases from approximately  $0.2 \text{ cm s}^{-1}$  at  $[\text{NO}_2] = 1 \text{ nmol mol}^{-1}$  to  $0.5 \text{ cm s}^{-1}$  at  $[\text{NO}_2] = 30 \text{ nmol mol}^{-1}$ . This  $\text{NO}_2$  deposition is equal to 6 to 20% of nighttime  $\text{NO}_y$  flux observed by eddy covariance at the site [Horii 2002].

The nighttime deposition of  $\text{NO}_2$  in the canopy is confirmed by observations of  $\text{NO}$ ,  $\text{NO}_2$ , and  $\text{O}_3$  concentration profiles at the main tower (Figure 3). Concentrations of  $\text{NO}$  above the canopy at night are very small, often below the instrumental detection limit and indistinguishable from zero. Nighttime  $[\text{NO}_x]$  profiles exhibit a deposition signature similar to  $\text{O}_3$ , with  $dC/dz > 0$ , notwithstanding the small soil emissions of  $\text{NO}$  at the site of  $\leq 0.9 \mu\text{mol m}^{-2} \text{ hr}^{-1}$  [Munger et al., 1996]. We compared the  $\text{NO}_x$  and  $\text{O}_3$  fluxes by inferring average eddy diffusivity,  $K$ , derived from the flux-gradient relationship for each species:  $F = -K dC/dz$ , using the measured eddy

covariance fluxes of  $\text{NO}_2$  and  $\text{O}_3$  above the canopy and the average concentration gradient between 5m and 24m. We found nighttime values of  $K \approx 2400 \text{ cm}^2 \text{ s}^{-1}$  with remarkable consistency:  $K_{\text{NO}_x}/K_{\text{O}_3}$  varied between 0.5 and 1.5 with a mean value  $\sim 1$  independent of season (April-August) and  $\text{NO}_x$  concentration.

Evidence for deposition to surfaces such as leaves, litter, bark, and soil, has been reported previously by Eugster and Hesterberg [1996] and Hanson and Lindberg [1991] (see also references therein). Hydrolysis of  $\text{N}_2\text{O}_5$  on forest surfaces below the sensor height is a possible mechanism (reactions (4)-(6)). The rate-limiting step is formation of  $\text{NO}_3$  in reaction (4) [e.g. Jacob, 2000]:



We estimated an upper limit for  $\text{NO}_2$  deposition due to this process by calculating production of  $\text{NO}_3$  in (4) from data for  $\text{O}_3$  and  $\text{NO}_2$  (Figure 3) and assuming 100% efficiency for reactions (5) and (6), and concluded that hydrolysis of  $\text{N}_2\text{O}_5$  accounts for at most a minor fraction ( $<30\%$ ) of the observed nighttime  $\text{NO}_2$  deposition.

Deposition of  $\text{NO}_2$  and the non-linear dependence of flux on concentration could also be explained by heterogeneous conversion to HONO and  $\text{HNO}_3$ , as observed on aerosols [Notholt et al., 1992]. The mechanisms and kinetics of the associated  $\text{NO}_2$  reactions on hydrated surfaces are not fully understood. Heterogeneous  $\text{NO}_2$  hydrolysis likely proceeds by the overall reaction



[Goodman et al., 1999]. Laboratory studies have shown first-order kinetics in  $\text{NO}_2$  for reaction (7) at  $\mu\text{mol mol}^{-1}$  (parts-per-million) concentrations, with  $\text{NO}_2$  adsorption as the rate-limiting

step, but the rate at low-concentrations on forest surfaces is unknown. The atmospheric mechanism is likely to involve formation of  $\text{N}_2\text{O}_4$  as an intermediate on the surface [Finlayson-Pitts et al., 2003]. As in the  $\text{N}_2\text{O}_5$  hydrolysis mechanism, the aqueous-phase  $\text{HNO}_3$  produced in (7) is not likely to be released to the gas phase, but HONO might be returned to the atmosphere.

Harrison et al. [1996] observed upward HONO fluxes over vegetated surfaces at  $\text{NO}_2$  concentrations above  $10 \text{ nmol mol}^{-1}$ , with a quadratic dependence of  $[\text{HONO}]$  on  $[\text{NO}_2]$ ; likewise, HONO measurements by Thornberry et al. [2001] are consistent with heterogeneous production from  $\text{NO}_2$ . If the observed  $\text{NO}_2$  flux at Harvard Forest is the result of (7), then approximately half could return to the atmosphere as gas-phase HONO. Since HONO is rapidly photolyzed to NO and OH, up to half the  $\text{NO}_2$  deposition would therefore not contribute to net loss of  $\text{NO}_x$  from the atmosphere. The possible heterogeneous HONO formation at the surface during the night is important to daytime  $\text{HO}_x$  chemistry, delivering a burst of OH and NO radicals to the surface layer at sunrise when HONO photolyzes.

*Daytime fluxes.* During daylight hours we observed large compensating fluxes, upward for  $\text{NO}_2$  and downward for NO (Figure 1); these are largely due to the influence of the forest canopy on the vertical  $\text{NO}_2$  photolysis gradient (Reaction 3) [Gao et al., 1993]. Higher irradiance above the canopy favors production of NO (reaction 2); lower light below the canopy shifts the balance toward  $\text{NO}_2$  (reactions 1a and 1b). The eddy covariance fluxes of NO and  $\text{NO}_2$  are correlated on an hourly basis during the daytime: an orthogonal distance fit yields  $F_{\text{NO}_2} = -(4.0 \pm 0.1)F_{\text{NO}}$ ,  $R^2=0.80$ . The exchange velocities for NO and  $\text{NO}_2$  follow light levels as measured by PPFD (Figure 4), as expected for gradients associated with photolysis (Figure 3). There is a seasonal change in the dependence of daytime  $\text{NO}_2$  flux on PPFD, correlated with canopy development, with a lower slope of the  $\text{NO}_2$  exchange velocity vs. PPFD for leafless

periods. This result is also consistent with the expected effect of a smaller above- to below-canopy light gradient under leafless conditions, although we cannot rule out a chemical or biological role in  $\text{NO}_2$  exchange for the leaves. Since PPFD is a commonly measured and modeled quantity, we make use of this quantity as a proxy for photochemical activity in a simple parameterization of  $\text{NO}_x$  flux at our site (see below).

The magnitude of the daytime upward flux of  $\text{NO}_2$  in Figure 1 is greater than the corresponding downward flux of  $\text{NO}$ , an artifact of the different sampling heights for  $\text{NO}$  (29 m on the main tower) and the TDLAS  $\text{NO}_2$  (22 m on the auxiliary tower). Gao et al. [1993] showed that the photochemical fluxes are very sensitive to height, and the coupled photochemical fluxes of  $\text{NO}$  and  $\text{NO}_2$  cancel exactly, making no contribution to net  $\text{NO}_x$  flux.

Global 2-D and 3-D models often parameterize  $\text{NO}_2$  flux using canopy resistances assumed similar to  $\text{O}_3$  [e.g. Wang et al., 1998; Wesely and Hicks 2000]. In light of the high concentrations used in studies suggesting stomatal control of  $\text{NO}_2$  [as discussed in Lerda et al. 2000], and recent results calling into question the dominance of stomatal control of  $\text{O}_3$  deposition to a forest canopy in the presence of biogenic hydrocarbons [Kurpius and Goldstein 2003], we adopted the hypothesis that photochemical  $\text{NO}$ - $\text{NO}_2$  cycling has no effect on deposition and represent it in our dataset by a simple light-dependent term. We then use a multiple regression to determine the most likely contributions of other processes to the net flux.

We represented fluxes of  $\text{NO}_2$  by the sum of terms with constant exchange velocity (as expected for  $\text{O}_3$ -like depositors), concentration-dependent exchange velocity (as observed at night), light-dependent photochemical cycling, and possible exchange processes under stomatal control. Stomatal conductance ( $g_c$ , calculated using the measured water vapor flux and the Penman-Monteith equation after Shuttleworth et al. [1984]) correlates with PPFD, but the diel

variations of the two differ in terms of morning/afternoon asymmetry and at dawn and dusk, making it possible to distinguish stomatally-controlled from simple light-dependent processes, if both are strong enough. Thus we parameterize the flux of NO<sub>2</sub>, 2m above the canopy, day and night, by the function:

$$FNO_2 = V_0 \cdot [NO_2] + a \cdot [NO_2]^2 + (b+f) \cdot PPFD \cdot [NO_2] + \gamma \cdot g_c \quad (8)$$

where  $f$  is added to the coefficient of PPFD to account for the observed difference between full-canopy and leaves-off conditions. The coefficients for  $FNO_2$ ,  $V_0$ ,  $a$ ,  $b$ , and  $f$ , (Table 1) are consistent whether they are computed from the full data set, or selected subsets (high [NO<sub>2</sub>], daytime, and nighttime). However, for low-NO<sub>2</sub> conditions some coefficients have low statistical significance. The coefficient  $\gamma$  is marginally significant in most of the fits and follows the expected behavior for a stomatal process with a compensation point. The  $\gamma \cdot g_c$  term appears to contribute a downward component of NO<sub>2</sub> flux when NO<sub>2</sub> is high (>2 nmol mol<sup>-1</sup>) and an upward flux when NO<sub>2</sub> is low (<1.5 nmol mol<sup>-1</sup>). Low-NO<sub>x</sub> conditions dominate at the site [Munger et al., 1996].

Fluxes of NO from soils at our site are measurable, but small. The major contributor to FNO during the day is the simple dependence on PPFD. We included a constant exchange velocity and a light-dependend term, giving the NO flux 7 m above the canopy as:

$$FNO = V_{0\_NO} \cdot [NO] + b' \cdot PPFD \cdot [NO]. \quad (9)$$

This parameterization indicates a small deposition velocity, with large fluxes due to photochemical cycling: using all available data (956 hours),  $R^2=0.92$ ,  $V_{0\_NO} = -0.25 \pm 0.02 \text{ cm s}^{-1}$ , and  $b' = -0.87 \pm 0.03 \text{ cm s}^{-1} (\mu\text{mol m}^{-2} \text{ s}^{-1})^{-1}$ .

Because net NO flux (soils and deposition) appear small, we estimated the net flux of NO<sub>x</sub> from FNO<sub>2</sub> (8) by omitting the photochemical cycling components:

$$FNO_x(\text{net}) \approx FNO_2 - (b+f) \cdot \text{PPFD} \cdot [\text{NO}_2] = V_0 \cdot [\text{NO}_2] + a \cdot [\text{NO}_2]^2 + \gamma \cdot g_c \quad (10)$$

Figure 5 illustrates the relative contributions of each term to net flux and the resulting net NO<sub>2</sub> exchange velocity, for all conditions and for high NO<sub>2</sub> periods, using the coefficients from Table 1, measured NO<sub>2</sub> concentrations, and calculated g<sub>c</sub>. When NO<sub>2</sub> concentrations are low during the day, NO<sub>2</sub> is *emiitted* under stomatal control, tending to compensate for NO<sub>2</sub> deposition. When NO<sub>2</sub> concentrations are high during the day, NO<sub>2</sub> is *deposited* under stomatal control, as much as doubling the rate of NO<sub>2</sub> deposition. For most conditions at Harvard Forest, non-stomatal deposition accounts for the largest fraction of the flux, during the night as well as the day. The daytime net NO<sub>x</sub> flux was ~2 % of total daytime NO<sub>y</sub> deposition during the summer [Horii 2002]. The lifetime of NO<sub>x</sub> associated with deposition, based on an average net NO<sub>x</sub> deposition velocity of 0.2 cm s<sup>-1</sup> and regionally representative mixed layer depths [Holzworth 1967], varies between 10 days in summer and 4 days in winter, assuming surface deposition continues throughout the year as it does from early spring through late fall. τ(NO<sub>x</sub> deposition) may decrease to less than 24 hours during shallow nighttime inversions. In comparison, the characteristic time for NO<sub>2</sub> oxidation by OH varies from less than 12 hours in summer to more than 5 days in winter [Munger et al., 1998]. Evidently direct NO<sub>x</sub> deposition to forest surfaces has the largest impact on tropospheric chemistry when mixing layer depths are shallow and when other oxidative processes are relatively slow.

The daytime NO<sub>x</sub> and O<sub>3</sub> profiles for April-August 2000 (Figure 3; representative of profiles observed between 1990 and 2002) are qualitatively consistent with the independent eddy covariance flux measurements and net NO<sub>x</sub> flux parameterization. Under low-NO<sub>x</sub> conditions, profiles have a weak gradient, implying a net NO<sub>x</sub> flux approaching zero, with non-stomatal deposition to the ground offset by apparent emission in the upper canopy; the persistent NO<sub>x</sub>

enhancement at 24m may correspond to stomatal or other UV-induced NO<sub>2</sub> emission reported from vegetation at ambient concentrations below 1 nmol mol<sup>-1</sup> [Hari et al., 2003]. The profiles indicate that net NO<sub>x</sub> deposition is stronger at higher [NO<sub>x</sub>] compared to lower [NO<sub>x</sub>], and during the summer compared to the early spring.

## CONCLUSION

Nighttime NO<sub>2</sub> flux at Harvard Forest is predominantly downward. Because N<sub>2</sub>O<sub>5</sub> hydrolysis is insufficient to account for the observed deposition flux, particularly at the highest NO<sub>2</sub> concentrations, mechanisms that may produce HONO could be important. Daytime fluxes of NO and NO<sub>2</sub> are strongly coupled and dominated by simple photochemical exchange that does not contribute to net NO<sub>x</sub> flux. We concluded that NO<sub>2</sub> and NO fluxes can be parameterized in terms of known physical processes to derive a deposition velocity for NO<sub>2</sub> of ~0.2 cm s<sup>-1</sup>. Stomatal influence is weaker than typically assumed in models, and it changes sign depending on NO<sub>2</sub> concentrations, with overall near zero deposition or emission in the daytime for NO<sub>x</sub> less than approximately 1.5 nmol mol<sup>-1</sup>, and significant stomatal uptake for high NO<sub>x</sub>. These results underscore the importance of including both non-foliar deposition and a compensation point in NO<sub>2</sub> surface exchange parameterizations embedded in models of tropospheric chemistry and transport. Overall, we have found by direct measurements in field conditions that vegetation serves as a net sink for NO<sub>x</sub> radicals, with the sink strength increasing as NO<sub>x</sub> rises above ~ 10 nmol/mol of air. Contrary to previous assumptions, the sink persists at night and in the dormant season.

**REFERENCES**

- Eugster, W. and R. Hesterberg, Transfer resistances of NO<sub>2</sub> determined from eddy correlation flux measurements over a litter meadow at a rural site on the Swiss plateau, *Atmos. Environ.* *30*, 1247-1254, 1996.
- Finlayson-Pitts, B. J., L. M. Wingen, A. L. Sumner, D. Syomin, and K. A. Ramazan, The heterogeneous hydrolysis of NO<sub>2</sub> in laboratory systems and in outdoor and indoor atmospheres: An integrated mechanism, *Phys. Chem. Chem. Phys.*, *5*, 223-242, 2003.
- Fitzjarrald, D. R. and D. H. Lenschow, Mean concentration and flux profiles for chemically reactive species in the atmospheric surface layer, *Atmos. Environ.* *17*, 2505-2512, 1983.
- Gao, W., M. L. Wesely, P. V. Doskey, Numerical Modeling of the Turbulent Diffusion and Chemistry of NO<sub>x</sub>, O<sub>3</sub>, Isoprene, and Other Reactive Trace Gases in and Above a Forest Canopy, *J. Geophys. Res.* *98*, 18339-18353, 1993.
- Goodman, A. L., G. M. Underwood, and V. H. Grassian, Heterogeneous Reaction of NO<sub>2</sub>: Characterization of Gas-Phase and Adsorbed Products from the Reaction, 2NO<sub>2</sub>(g) + H<sub>2</sub>O(a) → HONO(g) + HNO<sub>3</sub>(a) on Hydrated Silica Particles, *J. Phys. Chem. A* *103*, 7217-7223, 1999.
- Goulden, M.L, J.W. Munger, S.-M. Fan, B. C. Daube, and S. C. Wofsy, Measurements of carbon sequestration by long-term eddy covariance: Methods and a critical evaluation of accuracy, *Global Change Biology* *2*, 169-182, 1996.
- Hanson, P. and S. E. Lindberg, Dry deposition of reactive nitrogen compounds: a review of leaf, canopy, and non-foliar measurements, *Atmos. Environ.* *25A*, 1615-1634, 1991.
- Hari, P. M. Raivonen, T. Vesala, J. W. Munger, K. Pilegaard, M. Kulmala, Ultraviolet light and leaf emission of NO<sub>x</sub>, *Nature*, *422*, 134, 2003.
- Harrison, R. M., J. D. Peak, G. M. Collins, Tropospheric cycle of nitrous acid, *J. Geophys. Res.* *101*, 14429-14439, 1996.
- Hirsch, A. I., J. W. Munger, D. J. Jacob, L. W. Horowitz, and A. H. Goldstein, Seasonal variation of the ozone production efficiency per unit NO<sub>x</sub> at Harvard Forest, Massachusetts, *J. Geophys. Res.* *101*, 12659-12666, 1996.
- Holzworth, G. C., Mixing depths, wind speeds and air pollution potential for selected locations in the United States, *J. Appl. Meteorol.*, *6*, 1039-1044, 1967.
- Horii, C. V., Tropospheric Reactive Nitrogen Speciation, Deposition, and Chemistry at Harvard Forest, Doctoral Thesis, Harvard University, 2002.
- Horii, C. V., M. S. Zahniser, D. D. Nelson, J. B. McManus, S. C. Wofsy, Nitric Acid and Nitrogen Dioxide Flux Measurements: a New Application of Tunable Diode Laser Absorption Spectroscopy, *Proc. of SPIE*, *3758*, 152-161, 1999.

- Jacob, D. J., J. A. Logan, G. M. Gardner, R. M. Yevich, C. M. Spivakovsky, and S. C. Wofsy, Factors Regulating Ozone Export Over the United States and Its Export to the Global Atmosphere, *J. Geophys. Res.*, *98*, 14817-14826, 1993.
- Jacob, D. J., Heterogeneous chemistry and tropospheric ozone, *Atmos. Environ.* *34*, 2131-2159, 2000.
- Kurpius, M. R. and A. H. Goldstein, Gas-phase chemistry dominates O<sub>3</sub> loss to a forest, implying a source of aerosols and hydroxyl radicals to the atmosphere, *Geophys. Res. Lett.* *30*, 1371, 2003.
- Lefter, B. L., and R. W. Talbot, Nitric acid and ammonia at a rural northeaster U.S. site, *J. Geophys. Res.* *104*, 1645-1661, 1999.
- Lerdau, M. T., J. W. Munger, D. J. Jacob, The NO<sub>2</sub> Flux Conundrum, *Science* *289*, 2291-2293, 2000.
- Liang, J., L. W. Horowitz, D. J. Jacob, Y. Wang, A. M. Fiore, J. A. Logan, G. M. Gardner, and J. W. Munger, Seasonal budgets of reactive nitrogen species and ozone over the United States, and export fluxes to the global atmosphere, *J. Geophys. Res.*, *103*, 13435-13450, 1998.
- Liu, S. C., M. Trainer, F. C. Fehsenfeld, D. D. Parrish, E. J. Williams, D. W. Fahey, G. Hübler, and P. C. Murphy, Ozone Production in the Rural Troposphere and the Implications for Regional and Global Ozone Distributions, *J. Geophys. Res.* *92*, 4191-4207, 1987.
- Moody, J. L., J. W. Munger, A. H. Goldstein, D. J. Jacob, and S. C. Wofsy, Harvard Forest regional-scale air mass composition by Patterns in Atmospheric Transport History (PATH), *J. Geophys. Res.* *103*, 13181-13194, 1998.
- Munger, J. W., S. C. Wofsy, P. S. Bakwin, S-M. Fan, M. L. Goulden, B. C. Daube, and A. H. Goldstein, Atmospheric deposition of reactive nitrogen oxides and ozone in a temperate deciduous forest and a subarctic woodland: 1. Measurements and mechanisms, *J. Geophys. Res.* *101*, 12639-12657, 1996.
- Munger, J. W., S-M. Fan, P. S. Bakwin, M. L. Goulden, A. H. Goldstein, A. S. Colman, and S. C. Wofsy, Regional budgets for nitrogen oxides from continental sources: Variations of rates for oxidation and deposition with season and distance from source regions, *J. Geophys. Res.* *103*, 8355-8368, 1998.
- Notholt, J., J. Hjorth, and F. Raes, Formation of HNO<sub>2</sub> on aerosol surfaces during foggy periods in the presence of NO and NO<sub>2</sub>, *Atmos. Environ.* *26A*, 211-217, 1992.
- Rondon, A., C. Johansson, L. Granat, Dry Deposition of Nitrogen Dioxide and Ozone to Coniferous Forests, *J. Geophys. Res.* *98*, 5159-5172, 1993.
- Rothman, L. S., et al., "The HITRAN molecular spectroscopic database and HAWKS (HITRAN Atmospheric Workstation): 1996 Edition," *J. Quant. Spectrosc. Radiat. Transfer*, *60*, 665-710, 1998.

- Shuttleworth, W. J., J. H. C. Gash, C. R., Lloyd, C. J. Moore, J. Roberts, A. D. Marques, G. Fisch, V. D. Silva, M. D. G. Ribeiro, L. C. B. Molion, L. D. D. Sa, J. C. A. Nobre, O. M. R. Cabral, S. R. Patel, J. C. Demoraes, Eddy correlation measurements of energy partition for Amazonian forest, *Quart. J. R. Met. Soc.*, *110*, 1143-1162, 1984.
- Sparks, J. P., R. K. Monson, K. L. Sparks, M. Lerdau, Leaf uptake of nitrogen dioxide (NO<sub>2</sub>) in a tropical wet forest: implications for tropospheric chemistry, *Oecologia* *127*, 214-221, 2001.
- Thornberry, T., M. A. Carroll, G. J. Keeler, S. Sillman, S. B. Bertman, M. R. Pippin, K. Ostling, J. W. Grossenbacher, P. B. Shepson, O. R. Cooper, J. L. Moody, and W. R. Stockwell, Observations of reactive oxidized nitrogen and speciation of NO<sub>y</sub> during the PROPHET summer 1998 intensive, *J. Geophys. Res.*, *106*, 24359-24386, 2001.
- Taylor, B. N., *Guide for the Use of the International System of Units (SI)*, NIST Special Publication 811, U.S. Government Printing Office, Washington, DC, 1995.
- Wang, Y., D.J. Jacob, and J.A. Logan, Global simulation of tropospheric O<sub>3</sub>-NO<sub>x</sub>-hydrocarbon chemistry, 1. Model formulation, *J. Geophys. Res.*, *103/D9*, 10,713-10,726, 1998.
- Wesely, M. L., Parameterization of surface resistances to gaseous dry deposition in regional-scale numerical models, *Atmos. Environ.* *23*, 1293-1304, 1989.
- Wesley, M. L., and B. B. Hicks, A review of the current status of knowledge on dry deposition, *Atmos. Environ.* *34*, 2261-2282, 2000.
- Williams, E. J., G. L. Hutchinson, and F. C. Fehsenfeld, NO<sub>x</sub> and N<sub>2</sub>O emissions from soil, *Global Biogeochem. Cycles*, *6*, 351-388, 1992.

**CAPTIONS:**

**Figure 1:** Diel cycles of median concentrations (upper panels) and fluxes (lower panels) for the Northwest ( $270^{\circ}$ - $45^{\circ}$ , left panels) and Southwest ( $180^{\circ}$ - $270^{\circ}$ , right panels) wind sectors at Harvard Forest, April-November, 2000, for NO, NO<sub>2</sub>, and O<sub>3</sub> $\times 10^{-1}$ . NO and O<sub>3</sub> were sampled at a height of 29 m, and NO<sub>2</sub> at 22 m. Vertical bars indicate 25<sup>th</sup> and 75<sup>th</sup> percentiles for NO and NO<sub>2</sub> measurements. Note the negative (downward) fluxes for NO<sub>2</sub> at night, reversing during the day, and the higher concentrations of NO<sub>2</sub> at night versus midday.

**Figure 2:** (A) Nighttime hourly (dots) and median nightly (pluses) NO<sub>2</sub> flux vs. concentration. The curve represents the function  $F_{NO_2} = F_0 + V_0 [NO_2] + a [NO_2]^2$ , with coefficients derived from a least-squares fit to the hourly data. The flux is expressed in units of concentration times velocity ( $\text{nmol mol}^{-1} \text{ cm s}^{-1}$ ) in order to simplify the interpretation of the coefficients in the least-squares fit. Pressure and temperature corrections have been taken into account in the conversion from density to mixing ratio flux units.

**Figure 3:**

Mean profiles of NO<sub>2</sub> (squares, dashed lines), NO<sub>x</sub>=NO<sub>2</sub>+NO (circles, solid lines), and O<sub>3</sub> (diamonds, solid lines) during the day (open symbols) and night (solid symbols) on the main Harvard Forest tower. Upper panels include April and May data; lower panels show June, July, and August (September-November profiles are unavailable for this year). Left panels are limited to  $[NO_2] < 1.5 \text{ nmol mol}^{-1}$ , right to  $[NO_2] > 2 \text{ nmol mol}^{-1}$ . Note the clear influence of forest canopy development from spring to summer on the NO<sub>2</sub> profile at higher  $[NO_2]$ , and the masking of this effect at low  $[NO_2]$  by apparent canopy-level NO<sub>2</sub> emission.

**Figure 4:** Daytime emission velocities of NO<sub>2</sub> and NO vs. photosynthetic photon flux density (PPFD). Symbols are medians of hourly data binned by percentiles of above-canopy PPFD.

NO<sub>2</sub> flux data are segregated into full-canopy conditions from early June to mid-October, and leafless periods in April-May and October-November. Linear fits to binned median points:

$VNO_2(\text{leaves on}) = (-0.4 \pm 0.1) + (2.7 \pm 0.2)PPFD$ ,  $R^2 = 0.97$ ;  $VNO_2(\text{leaves off}) = (0.1 \pm 0.1) + (1.5 \pm 0.2)PPFD$ ,  $R^2 = 0.90$ ;  $VNO(\text{leaves on}) = (-0.42 \pm 0.07) + (-0.5 \pm 0.1)PPFD$ ,  $R^2 = 0.78$ . Mid-

summer leaf area index at Harvard Forest is approximately 3.4, whereas the area index for bare stems and twigs is only 0.9 [Harvard Forest Online Data Archive, <<http://www-as.harvard.edu/data/nigec-data.html>>].

**Figure 5:**

Individual contributing terms and the net NO<sub>2</sub> flux based on the coefficients in Table 1, measured [NO<sub>2</sub>], and calculated  $g_c$ . The shaded regions indicate reasonable bounds on the net flux: the upper bound is the 75<sup>th</sup> percentile of net FNO<sub>2</sub> calculated using the upper confidence limit of the coefficients; the lower bound is the 25<sup>th</sup> percentile calculated with the lower confidence limit of the coefficients. Panels on the left use all data and the corresponding coefficients from Table 1; those on the right use data hours when NO<sub>2</sub> > 2 nmol mol<sup>-1</sup> and the high NO<sub>2</sub> coefficients.

**Table 1:** Multi-factor regressions of NO<sub>2</sub> and NO flux data using all available hourly observations of [NO<sub>2</sub>], PPFD, FNO<sub>2</sub>, and FNO, and calculated stomatal conductance,  $g_c$ , at Harvard Forest, April-November 2000. Day-only and night-only regressions exclude dawn and

dusk. Note the overall consistency of direction and magnitude of statistically significant terms, with the exception of the coefficient of  $g_c$ , which changes sign between high and low- $\text{NO}_2$  conditions. Terms with  $p > 0.1$  are italicized. Units for each term are:  $V_0$  ( $\text{cm s}^{-1}$ );  $a$  ( $\text{nmol}^{-1} \text{mol cm s}^{-1}$ );  $b$  ( $\text{cm s}^{-1} (\mu\text{mol m}^{-2} \text{s}^{-1})^{-1}$ );  $f$  ( $\text{cm s}^{-1} (\mu\text{mol m}^{-2} \text{s}^{-1})^{-1}$ ) where  $f=0$  for leaves-on conditions;  $\gamma$  ( $\text{nmol mol}^{-1}$ ).

Figure 1.

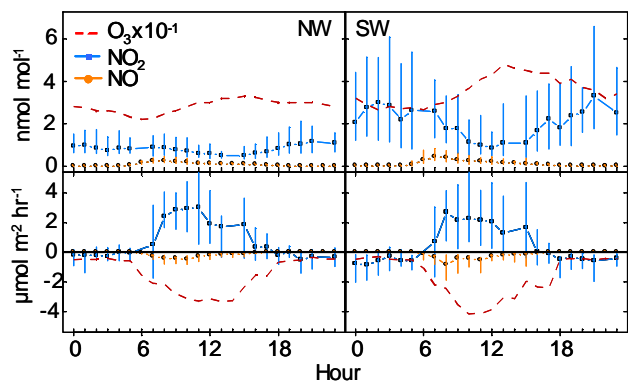


Figure 2.

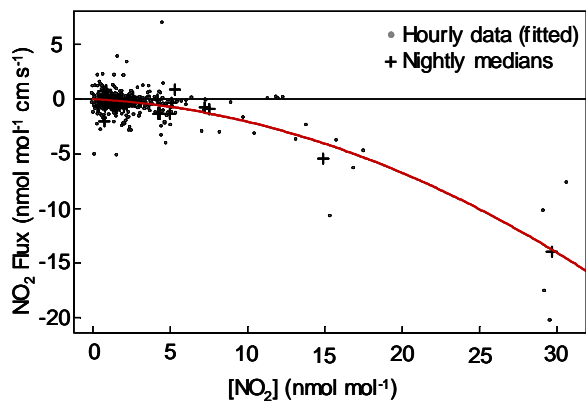


Figure 3.

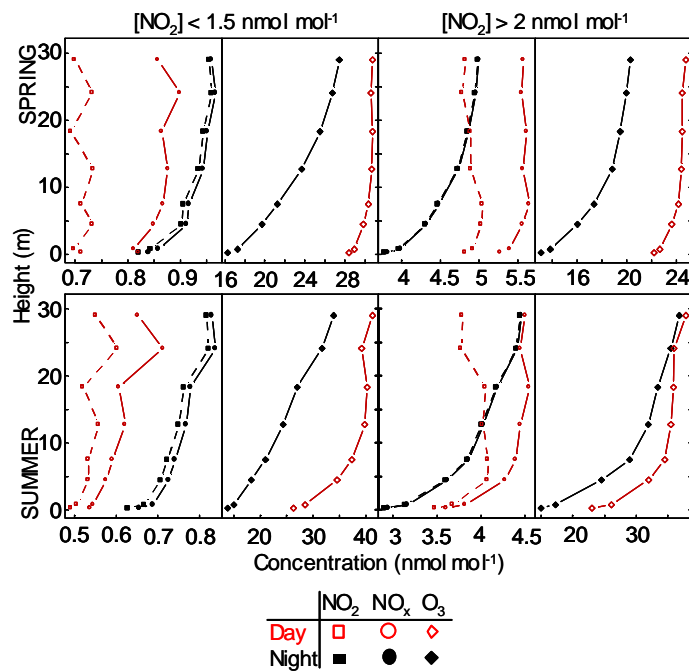


Figure 4.

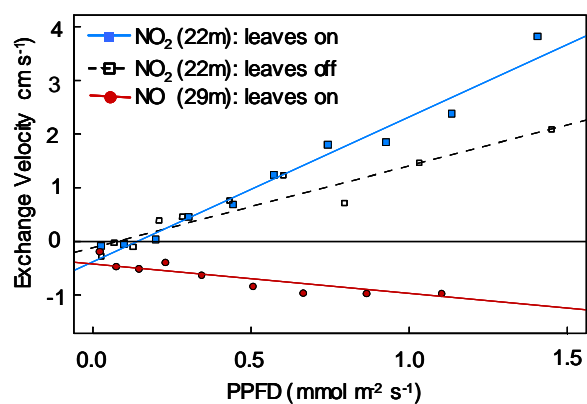


Figure 5.

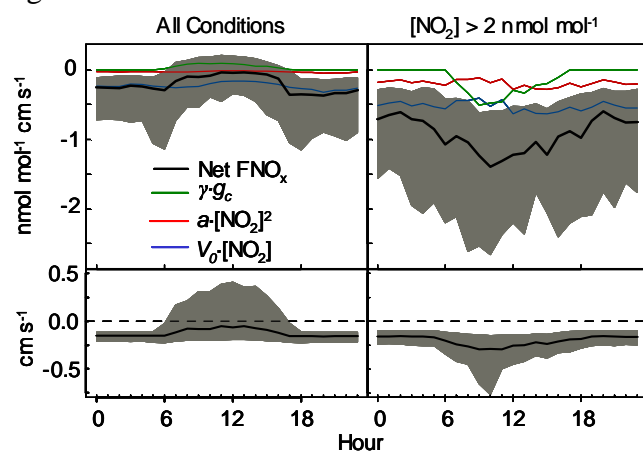


Table 1.

$z=22m: FNO_2 = V_0 \cdot [NO_2] + a \cdot [NO_2]^2 + (b+f) \cdot PPFD \cdot [NO_2] + \gamma \cdot g_c$					
	ALL DATA	$[NO_2] < 1.5$ nmol mol <sup>-1</sup>	$[NO_2] > 2$ nmol mol <sup>-1</sup>	DAY ONLY	NIGHT ONLY
	$R^2 = 0.60$	$R^2 = 0.15$	$R^2 = 0.75$	$R^2 = 0.63$	$R^2 = 0.60$
	N=928	N=464	N=306	N=412	N=316
$V_0$	$-0.14 \pm 0.03$	$-0.3 \pm 0.4$	$-0.12 \pm 0.04$	$-0.39 \pm 0.09$	$-0.08 \pm 0.03$
$a$	$-0.009 \pm 0.002$	$0.2 \pm 0.3$	$-0.010 \pm 0.002$	$0.008 \pm 0.009$	$-0.013 \pm 0.001$
$b$	$2.23 \pm 0.07$	$1.7 \pm 0.4$	$2.4 \pm 0.1$	$2.3 \pm 0.1$	NA
$f$	$-1.32 \pm 0.09$	$-1.2 \pm 0.5$	$-1.4 \pm 0.1$	$-1.3 \pm 0.1$	NA
$\gamma$	$0.2 \pm 0.2$	$0.8 \pm 0.4$	$-1.6 \pm 0.8$	$0.5 \pm 0.3$	NA